Formation and Growth of Ice Fog Particles at Fairbanks, Alaska

P. J. HUFFMAN[1]

Air Force Cambridge Research Laboratory
Bedford, Massachusetts 01730

T. OHTAKE[2]

Geophysical Institute, University of Alaska, College 99701

A mechanism is proposed for the formation of ice fog particles in the city and environs of Fairbanks, Alaska. Equations are developed for calculating the size distribution resulting from growth by deposition of water vapor. The equations are numerically solved with a computer for three major types of ice fog sources: (1) automobile exhaust, (2) exhaust from heating plants, and (3) open water. The size distribution produced by an individual source is determined by the cooling rate of water vapor injected into the environment. The cooling rate is a function of the source characteristics and the ambient temperature. The proposed mechanism adequately represents the observed size distribution if the cooling rate of the water vapor injected into the environment is not too large (source types 2 and 3). Because of the large cooling rate of the water vapor injected into the atmosphere by source type 1, the size distribution from this source is not adequately represented by the model. In agreement with observations, the computational results predict a decrease in the size of ice fog particles with decreasing ambient temperature for source types 2 and 3.

In an area as sparsely populated as interior Alaska, air pollution would appear to be an unlikely problem. During periods of clear sky, however, the long winter nights of the Arctic permit extreme radiative cooling of the earth's surface. In protected valley sites, this radiative cooling is often responsible for strong temperature inversions of extended duration [*Benson*, 1965]. One such location is the city and environs of Fairbanks.

At temperatures below −30°C, a large concentration of microscopic ice fog particles is normally present in the inversion layer. (The term 'ice fog particle' is used throughout to describe the elemental solid objects, regardless of shape, that compose the ice fog phenomenon. This nomenclature is used to distinguish ice fog particles from 'ice crystals,' the products of sublimation and freezing occurring in the higher atmosphere. Ice fog particles may be symmetrical but more often are irregular in shape. The term 'ice fog particle' does not imply a lack of crystal structure but refers rather to the mechanism of production.) The most prominent feature of ice fog is that it severely restricts visibility through the lowest part of the atmosphere. Ice fog is now most pronounced in and around Fairbanks, but it is a major problem in the development of interior Alaska and the arctic regions in general.

In the first detailed study of ice fog particles, *Thuman and Robinson* [1954] found that the mean statistical diameter decreases with decreasing temperature. At −40°C, the mean diameter of the irregular shaped particles, referred to as droxtals, is 13 μm. *Kumai* [1964] found that most ice fog particles are between 2 μm and 15 μm in diameter with a sharp peak in the distribution near 7 μm. More recent measurements [*Huffman*, 1968] show that the size distribution varies with location and often has more than one mode. Electron microscope analysis [*Ohtake*, 1967] reveals that the nuclei

[1] Now at Natural Resources Research Institute, University of Wyoming, Laramie 82070.

[2] On leave to Department of Atmospheric Science, Colorado State University, Fort Collins 80521.

of most ice fog particles are located well away from the geometric center and that many ice fog particles have no apparent nucleus at all. Recent measurements by *Henmi* [1969], who used *Ohtake*'s [1968] method, show that during ice fog conditions the ambient atmospheric water vapor content lies between the saturation values of water and ice.

Considerable theoretical attention has been given to the nucleation and growth of ice crystals in clouds [*Mason*, 1957; *Fletcher*, 1962; *Byers*, 1965]. This paper is a theoretical treatment of the nucleation and subsequent growth of ice fog particles. Water droplets and ice crystals form in the upper atmosphere, when the air cools gradually; throughout the growth period, the air mass is near the saturation level. On the other hand, we will show that ice fog particles are produced by the injection of saturated warm water vapor directly into a cold environment. Condensation takes place at a higher degree of supersaturation, and subsequent freezing occurs at much greater cooling rates. As the ice fog particles diffuse from their source of production, any remaining water droplets soon evaporate, causing further growth of existing ice fog particles by deposition and thus maintaining the environment near ice saturation.

THEORETICAL CONSIDERATIONS

If an exhaust gas containing water vapor at initial temperature T_i is injected into an environment at temperature T_0, $T_i \gg T_0$, the saturation ratio first increases as the gas begins to cool and then decreases as condensation proceeds. At any time, the saturation ratio S is given by

$$S = \frac{e}{e_s} \tag{1}$$

where e is the water vapor partial pressure, and e_s is the saturation vapor pressure at the same temperature. The time rate of change of the saturation ratio is thus

$$\frac{dS}{dt} = \frac{1}{e_s}\frac{de}{dt} - \frac{S}{e_s}\frac{de_s}{dt} \tag{2}$$

By using the ideal gas law for water vapor, the first term of (2) can be rewritten as

$$\frac{1}{e_s}\frac{de}{dt} = \frac{RT}{e_s M}\frac{d\rho_v}{dt} + \frac{S}{T}\frac{dT}{dt} \tag{3}$$

where R is the gas constant, T is the absolute temperature, M is the molecular weight of water, and ρ_v is the water vapor density. The time rate of change of water vapor density is

$$\frac{d\rho_v}{dt} = -\sum_i \frac{dm_i}{dt} - E \tag{4}$$

where m is the particle mass, and the summation is over all particles per unit volume. The term E in (4) takes into account the decrease in water vapor density due to entrainment of drier air from the environment caused by turbulence. The entrainment is greatest at the plume edge and penetrates further into the plume as the distance from the source increases. If the growth period of the ice fog particles is completed near the source (i.e., at a distance not much greater than the source diameter), the effect of entrainment will be negligible for particles formed well away from the plume edge. However, the growth mechanism near the plume edge will be altered by entrainment. By setting $E = 0$, the following treatment deals only with the central region of the exhaust plume where entrainment is minimal. The final computations reveal that the growth period is complete at distances of about 10, 50, and 100 cm, respectively, for automobiles, heating plants, and open water. For sources of typical cross-sectional area, we believe these distances to be small enough to justify the assumption that $E = 0$. By substituting (4), we can express (3) as

$$\frac{1}{e_s}\frac{de}{dt} = \frac{S}{T}\frac{dT}{dt} - \frac{RT}{e_s M}\sum_i \frac{dm_i}{dt} \tag{5}$$

The rate of change of saturation vapor pressure with time can be expressed as

$$\frac{de_s}{dt} = \frac{de_s}{dT}\frac{dT}{dt} = \frac{LMe_s}{RT^2}\frac{dT}{dt} \tag{6}$$

where the Clausius-Clapeyron equation for an ideal gas is used, and L is the latent heat of the phase change.

Inserting (5) and (6) into (2) gives

$$\frac{dS}{dt} = \frac{S}{T}\left(1 - \frac{LM}{RT}\right)\frac{dT}{dt} - \frac{RT}{e_s M}\sum_i \frac{dm_i}{dt} \tag{7}$$

For the temperatures of interest (233°K $\leq$

$T \leq 333°K$), LM/RT is already considerably greater than unity, and (7) can be simplified to

$$\frac{dS}{dt} = -\frac{LMS}{RT^2}\frac{dT}{dt} - \frac{RT}{e_s M}\sum_i \frac{dm_i}{dt} \qquad (8)$$

The appropriate values for e_s and L in (8) are the average values for the system of particles. Condensation first occurs to form water droplets that then freeze and continue to grow by sublimation. In general, the system consists of both water droplets and ice particles. On the basis of laboratory measurements of the freezing of distilled water drops, *Bigg* [1953] showed that the probability of freezing P, for a droplet of radius r, supercooled to a temperature T after t seconds is given by

$$\ln (1 - P) = -Ar^3 t(\exp T_s - 1)$$
$$T_s = 0 \qquad T > T_m$$
$$T_s = T_m - T \qquad T < T_m \qquad (9)$$

where A is a constant, and $T_m = 273°K$ is the melting temperature. *Langham and Mason* [1958], by using greatly refined purification methods, subsequently showed that the value of A in (9) depends on the particulate content of the water. However, when the water was completely particle free, giving rise to homogeneous freezing, the expression obtained was similar to (18) for homogeneous nucleation from the vapor phase. For water with particles, the results were explained as an exponential increase in the number of freezing nuclei with decreasing temperature.

Although, as discussed below, some ice fog particles are free of foreign particulate matter, most of them contain foreign aerosols that can serve as freezing nuclei. For this reason (9), with the value $A = 6.5 \times 10^{-4}$ cm^{-3} sec^{-1} taken from *Bigg* [1953], more nearly approximates the freezing function. (The validity of (9) for ice fog is doubtful because the literature refers to much lower cooling rates than those encountered here. The absolute temperature T, measured in the environment surrounding the particles, is nearly the same as the particle temperature only for sufficiently small cooling rates. However, because the values of e_s and L for ice do not differ greatly from the corresponding values for water, use of (9) for computing these parameters does not introduce appreciable error. Thus e_s and L have the form

$$e_s = e_w + \{1 - \exp [-Ar^3 t(e^{T_s} - 1)]\} \cdot (e_i - e_w) \qquad (10a)$$

$$L = L_v + \{1 - \exp [-Ar^3 t(e^{T_s} - 1)]\} \cdot (L_s - L_v) \qquad (10b)$$

where e_i and e_w, respectively, are the saturation vapor pressures over ice and water, and L_v and L_s, respectively, are the heats of vaporization and sublimation.

Three major types of ice fog sources are (1) automobile exhaust, (2) exhaust from heating plants (commercial and residential), and (3) open water. *Benson* [1965] showed that the rate of cooling of automobile exhaust along the centerline of the exhaust plume is given by the empirical relationship

$$\frac{dT}{dx} = -a(T - T_0)^2 \qquad T > T_0 \qquad (11)$$

where x is the distance from the source, and a is a constant. As expected, owing to similarities of the exhausting method, measurements of temperature profiles made during winter above several chimneys also fit the empirical curve (11). Air temperature measurements [*Ohtake*, 1968] indicate that the temperature gradient above open water can also be expressed by (11); the temperature drops from a value near 0°C at the water surface to the ambient value at a height of about 2 meters (we determined the value for a in each location by fitting (11) to the measured temperature profile). Thus, the theoretical aspects of ice fog formation from exhaust and from open water can be traced in the same mathematical manner, subject of course to different boundary conditions.

Integration of (11) gives the temperature as a function of distance from the source by

$$T = \frac{T_i - T_0}{(T_i - T_0)ax + 1} + T_0 \qquad (12)$$

Because the flow of the exhaust gas is turbulent, it will encounter a resistive drag force from the surrounding atmosphere that is proportional to the square of the flow velocity. The velocity of the exhaust gas as a function of distance from the source can therefore be expressed as

$$v = v_0 e^{-x/b} \qquad (13)$$

where v_0 is the initial velocity, and b is a constant, the value of which depends on the source characteristics. For automobile exhaust, v_0 and b were determined from empirical data [*Benson*, 1965]. Above open water, the updraft velocity is too small to be quantitatively measured but appears to be nearly constant up to several meters; we assumed its magnitude to be of the same order (several centimeters per sec) as the estimated uplift velocity of the frontal surfaces of cyclones [*Fletcher*, 1962; p. 5]. For (13) to give a nearly constant velocity with height, the value of b for open water was chosen 100 times larger than the empirically determined value for automobile exhaust. The correct choice of v_0 and b for heating plants is particularly difficult because no quantitative data of the velocity profile is available. However, we observed the initial velocity to be much less than that for automobiles. Also, compared with automobile exhaust, the velocity decreases more slowly with distance from the source. For the purpose of computation, v_0 and b for heating plant exhaust have been chosen respectively as 0.1 and 10 times the corresponding values for automobile exhaust.

Integrating (13) and substituting into (12) gives the temperature of an elemental volume of exhaust gas as a function of time by

$$T = \frac{T_i - T_0}{ab(T_i - T_0)\ln(ct + 1) + 1} + T_0 \quad (14)$$

where $c = v_0/b$. Figure 1 shows the temperature as a function of time given by (14) for the estimated values of a, b, T_i, and T_0.

Neglecting curvature and chemical effects, the diffusion growth rate of water droplets and ice crystals is usually given by the classical expression

$$\frac{dm}{dt} = \frac{4\pi C}{u + v}(S - 1)$$

$$u = \frac{L^2 M}{KRT^2} \qquad v = \frac{RT}{e_s DM} \quad (15)$$

where C is the capacitance of the particle in air, K is the thermal conductivity of air, and D is the diffusivity of water vapor in air. Equation 15 is not strictly correct when the growth rate is appreciable. If it is assumed, for mathematical simplicity, that the particle is approximately spherical throughout the growth period, the growth rate can be expressed more correctly [*Rooth*, 1957] by

$$\frac{dm}{dt} = \frac{4\pi}{u + v}(S - 1)\frac{r^2}{f + r} \quad (16)$$

where f is a correction term that takes into account the kinetics of vapor molecules and the accommodation coefficient of the particle surface. The exact value of f as a function of temperature is not known for water or ice because information regarding the variation of the accommodation coefficient is incomplete. We

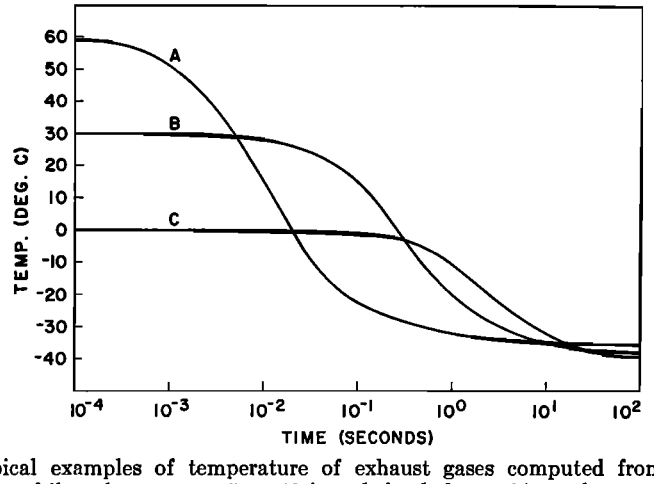

Fig. 1. Typical examples of temperature of exhaust gases computed from equation 14. Curve A: automobile exhaust, $a = 5 \times 10^{-4}$ cm^{-1} deg^{-1}, $b = 66.7$ cm^{-1}, $v_0 = 2000$ cm sec^{-1}. Curve 8: exhaust from heating plant, $a = 2 \times 10^{-4}$ cm^{-1} deg^{-1}, $b = 667$ cm^{-1}, $v_0 = 200$ cm sec^{-1}. Curve C: above open water, $a = 5 \times 10^{-4}$ cm^{-1} deg^{-1}, $b = 6670$ cm^{-1}, $v_0 = 20$ cm sec^{-1}.

chose the value $f = 5$ μm on the basis of the measured value of the condensation coefficient at 10°C and 1000 mb [*Alty and Mackay*, 1935]. Especially during the initial stages when r is small, f slows the growth process. The exact value chosen for f does not greatly affect the numerical results to be presented later in this section. For example, reducing f to zero results in about a twofold increase in the final results. By using (16), the summation in (8) can be expressed as

$$\sum_i \frac{dm_i}{dt} \rightarrow \frac{4\pi}{u+v}(S-1) \cdot \int_0^t I(t_n) \frac{r^2(t_n, t)}{f + r(t_n, t)}\, dt_n \qquad (17)$$

where $I(t_n)$ is the rate of formation of embryo droplets per unit volume at time t_n. Thus $r(t_n, t)$ is the radius at time t of particles formed at time t_n.

The cooling rates (Figure 1) are large enough to produce the degree of supersaturation required for homogeneous nucleation. Electron microscopy also reveals that ice fog particles are possibly nucleated homogeneously because some of the particles did not contain large nuclei in their replicas [*Ohtake*, 1967]. With the replica method, it is normally difficult to produce very clean supporting films. Even though we tried hard to make cleaner films for this purpose, so far most ice fog particle replicas contained very small nuclei or contaminations. However, many ice fog particles taken at Chena Hot Springs, where there is a much smaller amount of air pollution, lacked nuclei or contamination in the replicas. Also, the aerosol possibly could have been captured by an existing droplet previously nucleated homogeneously, and the presence of any foreign matter has no effect on the nucleation process. The homogeneous rate of embryo formation [*Farley*, 1952] is given by

$$I = \frac{e_s^2 S^2}{R^2 T^2}\left(\frac{2\eta^3 M\sigma}{\pi}\right)^{1/2} \exp\left\{-\frac{16\pi\eta M^2\sigma^3}{3R^3T^3 \ln^2 S}\right\} \qquad (18)$$

where σ is the surface tension of water, and η is Avagrado's number. The values of σ are for a flat water surface against air at the appropriate temperature T (values from *Handbook of Chemistry and Physics*, 41st edition; values below −8°C by extrapolation). It is apparent from (18) that the rate of embryo formation is very sensitive to the surface tension, and inaccuracies in σ resulting from surface curvature or lack of low temperature data could introduce significant error in the calculated values for I. The use of (18) for homogeneous nucleation of the liquid from the vapor phase and the use of (9) for the nucleation of ice from the liquid phase in the presence of foreign particulate matter is not inconsistent if it is assumed that such particulate matter is captured after the droplet is nucleated and before freezing occurs. Because of the high concentration of particulate pollutants normally present during ice fog conditions [*Benson*, 1965], this assumption is not unreasonable.

The set of (8), (14), (17), and (18), with e_s and L determined by (10*a*) and (10*b*), can be solved numerically to give the resulting size distribution as a function of the source parameters and the ambient temperature.

Comparison with Experiment

A computer programmed to calculate the saturation ratio as a function of time gave the results shown in Figure 2 for the three cooling rates of Figure 1. The exhaust gas is assumed to be initially saturated with respect to water, and the environment is assumed to be saturated with respect to ice. The fact that automobile and heating plant exhaust is initially saturated is justified by the fact that considerable cooling already takes place between the point of combustion and the exhaust exit, and water vapor is condensed on the walls of the exhaust system. From the time dependence of S, we evaluated the size distribution by calculating $I(t_n)$ versus $r(t_n, t)$ in the limit as t becomes large without bound. Figure 3 shows the size distribution obtained in this manner.

It must be remembered that we have considered only growth by diffusion. The 0.5-μm peak represented by curve A of Figure 3 could be shifted toward a larger diameter by coalescence. Calculations show that the maximum rate of droplet production is of the order of 10^{11} cm^{-3} sec^{-1}. Even with such a high concentration of embryo droplets and even under the assumption of a coalescence efficiency of 100% (a factor difficult to justify), the collision frequency be-

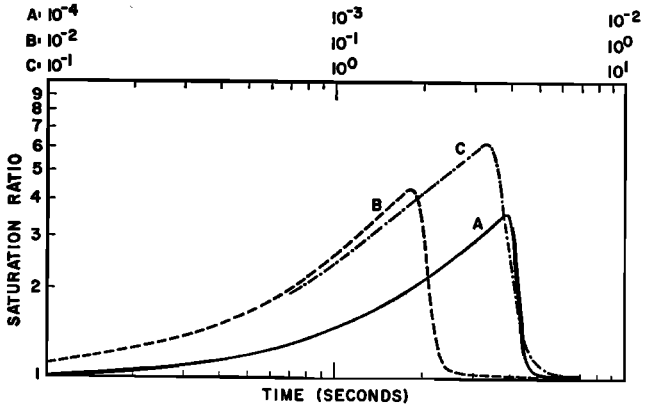

Fig. 2. Saturation ratio versus time for the cooling rates of Figure 1.

tween droplets due to Brownian motion would not be sufficient for appreciable growth by coalescence during the short time period available. However, because of the small size of the particles represented by curve A of Figure 3, probably only a few of them freeze if the ambient temperature is not too low ($T_0 > -40°C$); these may then grow to a diameter of several micrometers at the expense of the more numerous evaporating liquid droplets. By

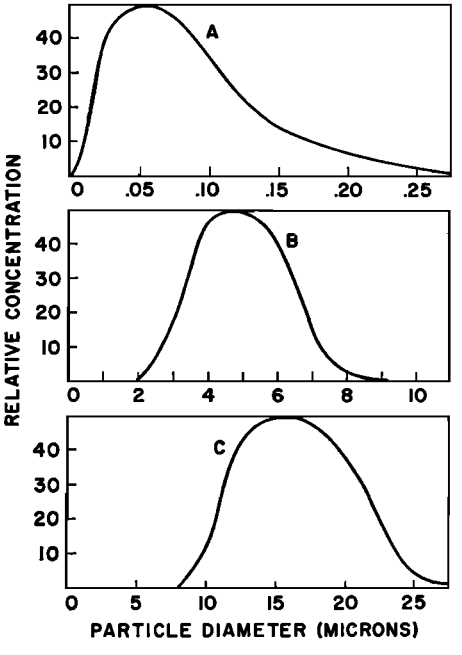

Fig. 3. Computed size distributions for ice fog particles produced by the cooling rates shown in Figure 1.

treating the growth of water drops and ice crystals in the same equation, the computational method developed adequately treats the growth problem only if the probability of freezing is large (i.e., if the initial droplets formed by condensation all freeze at nearly the same time, or if the particles are formed directly by deposition). If the probability of freezing is small (i.e., if only a few of the droplets freeze), the method fails to adequately distinguish between water droplets and frozen particles. The frozen particles grow faster than the liquid droplets because the saturation vapor pressure is lower for ice than for water. In fact, eventually in the growth period the saturation ratio falls below unity for the small liquid droplets and they evaporate, liberating additional water vapor for further growth of frozen particles. If the system consists predominantly of liquid droplets, the few existing ice fog particles can grow appreciably by this process. On the other hand, the larger particles represented by curves B and C of Figure 3 probably nearly all freeze very soon after their information; and, thus, in contrast to the previous case, there is not a large amount of excess water vapor available from liquid droplets to provide for rapid growth by deposition.

If the ambient temperature is very low ($T < -40°C$), it might be expected theoretically that even the very small droplets produced by source Type 1 would all freeze soon after formation. However, even after freezing such small dropets may in time evaporate in an environment near ice saturation because of the effect of surface curvature on the saturation

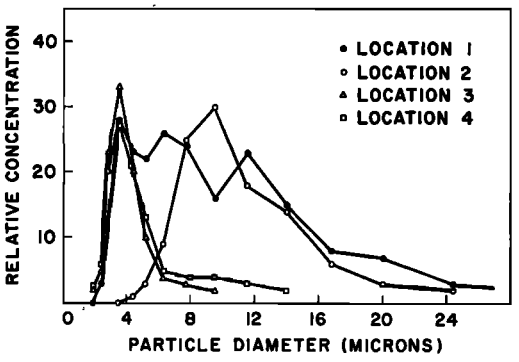

Fig. 4. Ice fog particle size distributions measured in the vicinity of Fairbanks, Alaska (see Figure 5 for location numbers).

vapor pressure. Sampling techniques, including electron microscopy [*Ohtake*, 1967], have failed to detect the existence of ice fog particles less than 1 μm in size even at ambient temperatures well below −40°C.

Figure 4 presents typical experimental ice fog particle size distributions obtained by impaction at several locations (see Figure 5) in the vicinity of Fairbanks, Alaska, at temperatures between −32°C and −40°C [*Huffman*, 1968]. Location 1 is in the downtown area. The Chena River adjacent to location 2 is always free of an ice cover owing to the operation of an electric power plant slightly upstream. Locations 3 and 4 are near airport facilities. The shape of the distribution at each location is usually (but not always) as shown in Figure 4, although the position of the peaks may be shifted by one or two micrometers.

The experimental results presented in Figure 4 compare favorably with the computed size distributions for source Types 2 and 3. The observed sizes of the ice fog particles produced by source Type 1 are much larger than the computed values owing, we believe, to the preferential growth of ice particles at the expense of water droplets as discussed above. The usual occurrence of a trimodal distribution at location 1 in the downtown area with peaks near 3.5, 6, and 12 μm diameter is believed due to the prevalence of the three types of ice fog sources: automobile exhaust, exhaust from heating plants, and open water, respectively. At location 2, the distribution is dominated by a single broad peak near 10 μm diameter. We expect this peak to be that of ice fog particles produced by open water of the Chena River. The occurrence of a single narrow peak of 3.5

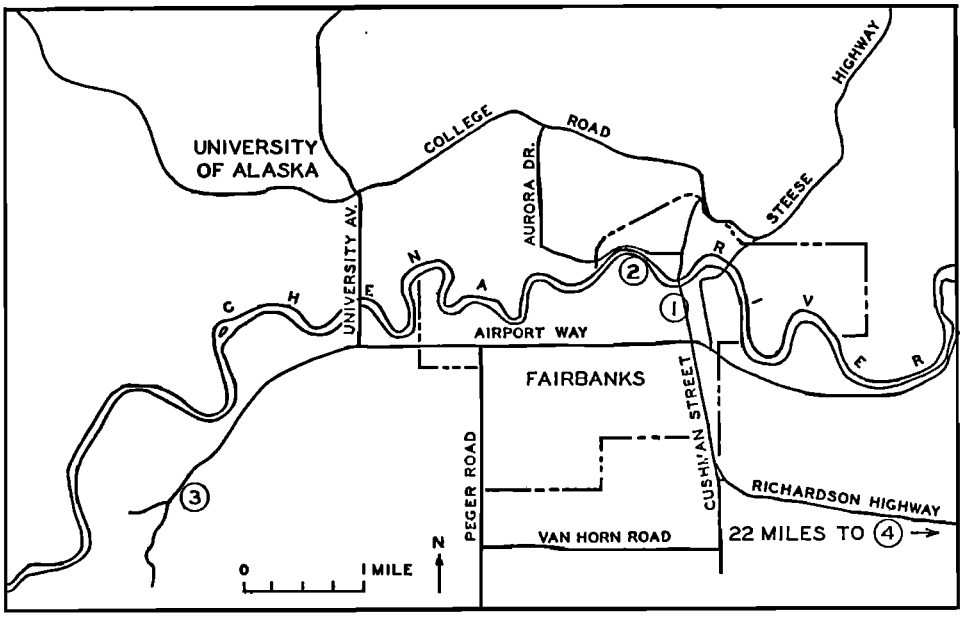

Fig. 5. Map showing locations where ice fog particles size distribution data were obtained. 1, Municipal Utilities System; 2, Industrial Air Products Co.; 3, Fairbanks Airport; 4, Eielson Air Force Base.

μm diameter at locations 3 and 4 is attributed to automobile and aircraft exhaust.

CONCLUSIONS

The chief factor influencing the size of ice fog particles produced by an individual source is the cooling rate of the exhaust gas determined by the source parameters a, b, v_0, and T_t, and the ambient temperature T_0. The model presented adequately represents the growth mechanism if the probability of freezing is large for the droplets initially formed by condensation, or if the growth occurs directly by deposition from the vapor phase. If, however, the probability of freezing is small, the treatment fails to adequately represent the growth mechanism. Because the probability of freezing can be expected to decrease for smaller droplet sizes, the treatment fails to adequately represent the growth mechanism if the initial droplets formed by condensation are too small. Thus, although the size distributions produced by heating plants and open water (source Types 2 and 3) are adequately represented by the model, the model fails to adequately represent the growth mechanism responsible for the development of ice fog particles from automobiles (source Type 1).

The most likely cause of the discrepancy between the observed and computed size distributions (other than that discussed above) is an incorrect assumption for the source velocity, equation 13, or somewhat incorrect choices for one or more of the values for the parameters a, b, v_0, T_t. Because the values for these parameters vary considerably among sources of the same type, and because at present the available experimental data are limited, the values chosen may not be typical. Furthermore, the entrainment of drier air from the environment limits the supply of water vapor available and alters the particle growth rate, particularly near the edge of the exhaust plume. The significance of this entrainment may be greater than assumed.

Other parameters being constant, the mean size of ice fog particles decreases as the temperature difference ($T_t - T_0$) becomes greater. On this basis one can expect a shift in the size distribution toward smaller diameters as the ambient temperature decreases. Although there is no simple relationship between the mode diameter and ambient temperature, numerical computations at other values of T_0 between -30°C and -40°C reveal the change is approximately linear with a rate constant of about 1 μm per 10°. Our experimental observations revealed no detectable change in size with ambient temperature indicating that any such change is indeed small, in agreement with the computational results. *Thuman and Robinson* [1954] and *Henmi* [1969] observed a variation comparable to our computational value for nearly spherical particles but report rates 10 to 20 times larger for other particle shapes. It is likely that the particles these researchers classify as spherical, which are in the same size domain as our experimental values, are those formed by the mechanism postulated here (freezing of condensed water droplets), whereas the other shapes, which are larger in size and fewer in number, may be associated with another mechanism of production (i.e., growth by deposition in the environment).

Perhaps further comment on the nucleation of ice fog particles is in order. We assumed that nucleation occurs homogeneously from the vapor to the liquid phase. Certainly much particulate matter is ejected by exhaust sources along with water vapor, and much of this particulate matter is capable of serving as condensation nuclei. A thorough study of the nucleation process must include detailed information of the active heterogeneous nuclei concentration near the source as a function of temperature and saturation ratio. However, if no heterogeneous nuclei were present, the cooling rates encountered are sufficient to cause the degree of supersaturation required for homogeneous nucleation; therefore, it is water vapor that is of primary importance in the formation of ice fog. In fact, the cooling rates are so rapid that even the presence of large concentrations of heterogeneous nuclei should not be expected to quench the rapidly rising supersaturation before the critical value for homogeneous nucleation is reached. In general, then, both homogeneous and heterogeneous nucleation should be effective.

Acknowledgments. The programming required for the numerical computations was performed by Mr. T. Spuria of Analysis and Computer Systems, Inc., Burlington, Massachusetts.

The research was supported in part by the National Center for Air Pollution Control, De-

partment of Health, Education and Welfare, Public Health Service, under grant AP 0049.

REFERENCES

Alty, T., and C. A. Mackay, The accommodation coefficient and the evaporation coefficient of water, *Proc. Roy. Soc., A, 199,* 104–116, 1935.

Benson, C. S., Ice fog: Low temperature air pollution, *Geophysical Institute Rep.* UAG R-173, 43 pp., (DDC No. 631553), 1965.

Bigg, E. K., The supercooling of water, *Proc. Phys. Soc., B, 66,* 688–694, 1953.

Byers, H. R., *Elements of Cloud Physics,* 191 pp., University of Chicago Press, Chicago, 1965.

Farley, F. J. M., The theory of the condensation of super-saturated ion-free vapor, *Proc. Roy. Soc., A, 212,* 530–542, 1952.

Fletcher, N. H., *The Physics of Rain Clouds,* 386 pp., Cambridge University Press, London, 1962.

Henmi, T., Some physical phenomena associated with ice fog, M.S. Thesis, University of Alaska, College, 1969.

Huffman, P. J., Size distribution of ice fog particles, M. S. thesis, University of Alaska, College, 1968.

Kumai, M., A study of ice fog and ice fog nuclei at Fairbanks, Alaska, *CRREL. Res. Rep.* 150, part I (DDC AD451667), 1964.

Langham, E. J., and B. J. Mason, The heterogeneous and homogeneous nucleation of supercooled water, *Proc. Roy. Soc., A, 247,* 493–504, 1958.

Mason, B. J., *The Physics of Clouds,* 481 pp. Clarendon Press, Oxford, 1957.

Ohtake, T., Alaskan ice fog, *Phys. Snow Ice,* part 1, Hokkaido University, Sapporo, 105–118, 1967.

Ohtake, T., Freezing of water droplets and ice fog phenomena, *Proc. Int. Conf. Cloud Phys.,* 285–289, 1968.

Rooth, C., On a special aspect of the condensation process and its importance in the treatment of cloud particle growth, *Tellus, 9,* 372–377, 1957.

Thuman, W. C., and E. Robinson, Studies of Alaskan ice-fog particles, *J. Meteorol., 11,* 151–156, 1954.

(Received March 20, 1970;
revised October 14, 1970.)